

# Tunable Superconducting Qubits with Flux-Independent Coherence

M. D. Hutchings,<sup>1</sup> J. B. Hertzberg,<sup>2</sup> Y. Liu,<sup>1</sup> N. T. Bronn,<sup>2</sup> G. A. Keefe,<sup>2</sup> J. M. Chow,<sup>2</sup> and B. L. T. Plourde<sup>1</sup>

<sup>1</sup>*Syracuse University, Department of Physics, Syracuse, NY 13244, USA*

<sup>2</sup>*IBM, TJ Watson Research Center, Yorktown Heights, NY 10598, USA*

(Dated: December 3, 2024)

We have studied the impact of low-frequency magnetic flux noise upon superconducting transmon qubits with various levels of tunability. We find that qubits with weaker tunability exhibit dephasing that is less sensitive to flux noise. This insight was used to fabricate qubits where dephasing due to flux noise was suppressed below other dephasing sources, leading to flux-independent dephasing times  $T_2^* \sim 15 \mu\text{s}$  over a tunable range of  $\sim 340$  MHz. Such tunable qubits have the potential to create high-fidelity, fault-tolerant qubit gates and fundamentally improve scalability for a quantum processor.

Quantum computers have the potential to outperform classical logic in important technological problems. A practical quantum processor must be comprised of quantum bits (“qubits”) that are isolated from environmental decoherence sources yet easily addressable during logical gate operations. Superconducting qubits are an attractive candidate because of their simple integration with fast control and readout circuitry. In recent years, advances in superconducting qubits have demonstrated how such integration may be achieved while maintaining high coherence [1–3]. Further extensions of qubit coherence will serve to reduce gate errors, cutting down the number of qubits required for fault-tolerant quantum logic [4, 5].

An important aspect of maintaining high qubit coherence is the reduction of dephasing. Frequency-tunable qubits are inherently sensitive to dephasing via noise in the tuning control channel. Tuning via a magnetic flux thus introduces dephasing via low-frequency flux noise [6–13]. Such noise is ubiquitous in thin-film superconducting devices at low temperatures. Experiments indicate a high density of unpaired spins on the thin-film surface [14] with fluctuations of these leading to low-frequency flux noise that typically has a  $1/f$  power spectrum [13, 15–17]. For any flux-tunable qubit, this flux noise leads to significant dephasing whenever the qubit is biased at a point with a large gradient of the qubit energy with respect to flux.

Flux tuning is nonetheless highly advantageous for many quantum circuits, and several classes of quantum logic gates rely on flux-tunable qubits. In the controlled-phase gate [1, 18], qubit pairs are rapidly tuned into resonance to create entanglement. Here, both flux noise and off-resonant coupling to other qubits produce phase errors proportional to gate times, with total gate error scaling as the square of the gate time [19]. Alternatively, fixed-frequency qubits have been employed in schemes such as the cross resonance (CR) gate [20, 21] to demonstrate aspects of quantum error correction (QEC) [3, 22]. Recent efforts with two-qubit devices have extended CR gate fidelities beyond 99% [23]. Larger lattices of fixed-frequency qubits, however, are likely to suffer increas-

ingly from frequency crowding. If a qubit’s 0-1 excitation frequency overlaps with the 0-1 or 1-2 frequency of its neighbor, or if the two qubits’ frequencies are very far apart, the CR gate between these two qubits will be non-ideal, with the strong possibility of leakage out of the computational subspace, or a very weak gate, respectively [24]. However, fixed-frequency transmon qubits are challenging to fabricate to precision better than about 200 MHz [25]. Given such imprecision, a hypothetical seventeen-qubit logic circuit could see up to a quarter of its gate pairs fail due to frequency crowding (see Supplement). Frequency-tunable transmon qubits therefore appear attractive for use in architectures based on the CR gate.

In this Letter, we show how a tunable qubit’s sensitivity to flux noise may be reduced by limiting its extent of tunability. We report results for several different qubits showing that the qubit dephasing rate is proportional to the sensitivity of the qubit frequency to magnetic flux and to the amplitude of low-frequency flux noise. Furthermore, we use the understanding gained through this study to fabricate a qubit whose dephasing due to non-flux dependent sources exceeds its dephasing due to low-frequency flux noise, over a range of more than 300 MHz of tunability. This unique qubit has the potential to reduce errors in gates employing frequency-tunable qubits and to evade frequency crowding in qubit lattices employing CR gates. It therefore offers a promising route to create high-fidelity two-qubit gates that reach fault-tolerant gate operation and to improve the scalability of superconducting qubit devices.

Our device adapts a design in which a superconducting quantum interference device (SQUID) serves as the Josephson inductance in a transmon qubit [26]. Here, the Josephson energy, and consequently the qubit 0-1 transition frequency  $f_{01}$ , may be tuned with a magnetic flux  $\Phi$  with a period of  $\Phi_0 \equiv h/2e$ , the magnetic flux quantum, where  $h$  is Planck’s constant and  $e$  is the electron charge. However, if the two junctions in the SQUID have different Josephson energies  $E_{J1}$  and  $E_{J2}$ , a so-called ‘asymmetric transmon’ is formed [27]. The greater the difference in junction energies, the smaller the level of tunability. If

$E_{J1} > E_{J2}$ , we can define the ratio  $\alpha = E_{J1}/E_{J2}$  and the sum  $E_{J\Sigma} = E_{J1} + E_{J2}$ . The total flux-dependent Josephson energy  $E_J$  varies according to the following expression from ref [26]:

$$E_J(\Phi) = E_{J\Sigma} \cos\left(\frac{\pi\Phi}{\Phi_0}\right) \sqrt{1 + d^2 \tan^2\left(\frac{\pi\Phi}{\Phi_0}\right)}, \quad (1)$$

where  $d$  is given by  $d = (\alpha - 1)/(1 + \alpha)$ .

To explore the dephasing behavior of qubits having such tunability, we prepared transmon qubits on two styles of chip, referred to as sample A and sample B. Both samples employ a multi-qubit planar circuit quantum electrodynamics (cQED) architecture with eight separate cavity/qubit systems. Qubits on the same chip should experience the same flux noise level, allowing a comparison of dephasing properties between them. On sample A, the eight frequency-multiplexed cavities are all coupled to a common feedline for microwave drive and readout (sample details and layout shown in Supplement). On this chip, we compare transmons having junction ratios  $\alpha = 7, 4, 1$  and a fixed-frequency single-junction qubit. We design for a particular  $\alpha$  by varying the junction areas in the SQUID, since  $E_J$  of a junction is directly proportional to its area. For consistency, the single-junction qubit maintained the same SQUID loop structure with one of the junctions being left open, and all four qubit types were designed to have the same  $E_{J\Sigma}$ . Sample B employs a qubit design similar to that in [3, 22, 28, 29]. For this device, all qubits have separate drive and readout microwave lines (layout shown in Supplement). Six qubits were designed to have  $\alpha = 15$  while two employed a single junction matching the  $E_{J1}$  of the tunable qubits. The fixed-frequency qubits act as a reference for non-flux dependent dephasing on each chip.

We used standard photolithographic and etch processes to pattern the coplanar waveguides, ground plane, and qubit capacitors from Nb sputtered films on Si substrates, followed by electron-beam lithography and deposition of conventional Al-AlO<sub>x</sub>-Al shadow-evaporated junctions. While all qubits were similar in design to [3, 22, 23], the transmon capacitor pads and SQUID loop geometry differed somewhat between samples A and B. Designs are shown in Fig. 1. Each sample was mounted on a dilution refrigerator in its respective lab (sample A at Syracuse; sample B at IBM) and surrounded by both room-temperature and cryogenic magnetic shields. Measurements for both samples were performed using standard cQED readout techniques [30]. Flux bias was applied to each sample during measurement using a wire coil placed close to the top of each device. Fabrication details and a discussion of measurement techniques are given in the Supplement.

Here we present data from four qubits on sample A and two qubits on sample B, one of each variation from

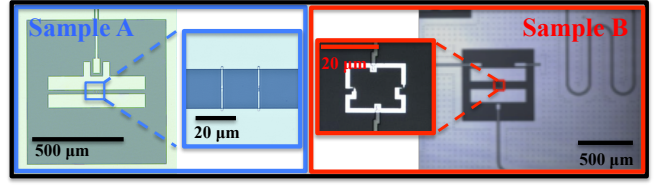


FIG. 1. (color online) Optical micrographs of example qubits from samples A and B.

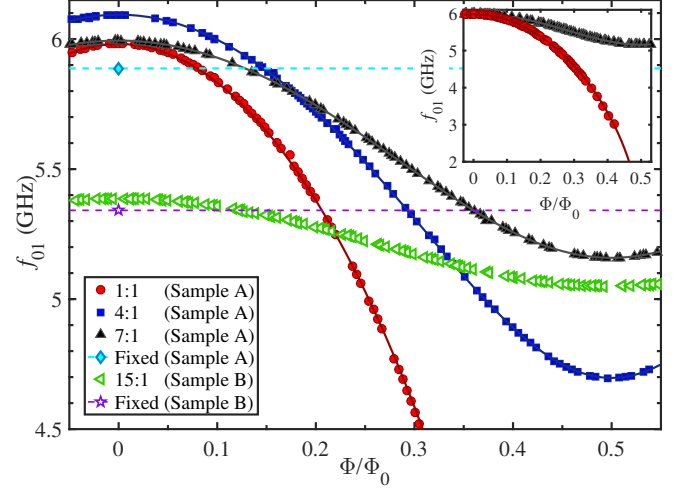


FIG. 2. (color online)  $f_{01}$  vs. flux measured for qubits from samples A and B. Solid lines are fits to these tuning curves based on Eq. 1. Also included are frequencies of single junction qubits from both samples. Dashed lines for these qubits to guide the eye. Inset: entire tuning range measured for the  $\alpha = 1$  qubit with the  $\alpha = 7$  qubit included as a comparison to illustrate the large frequency tunability of an  $\alpha = 1$  qubit.

each sample. Figure 2 shows the flux dependence of  $f_{01}$  for each qubit. We have subtracted any fixed flux offset appearing in the measurement. The  $\alpha = 15$  qubit on sample B had the weakest tunability of these: 337 MHz. Following Eq. (1) and the expectation that  $f_{01} \propto \sqrt{E_J}$  [26], we fit the data in Fig. 2 to find the maximum frequency  $f_{01}^{\max} \propto \sqrt{E_{J\Sigma}}$  and asymmetry parameter  $d$ . From the latter we compute  $\alpha$  for all tunable qubits and we find that the measured asymmetry  $\alpha$  was within 5% of the designed value. We note that the four sample A qubits shown in Fig. 2 were designed to have identical  $E_{J\Sigma}$  and therefore identical  $f_{01}^{\max}$ , but in fact exhibit a  $\sim 200$  MHz spread, thus illustrating the challenge of fabricating qubits to precise frequencies.

To assess the effect of flux noise on dephasing, we observe how the latter relates to each qubit's frequency gradient as a function of flux  $D_\Phi = \partial f_{01}/\partial \Phi$ . We characterize dephasing via measurement of the Ramsey decay time  $T_2^*$ , which is sensitive to low-frequency dephasing noise [7, 9]. We fit these using an exponential form. Although it has been shown that a dephasing noise source with

a  $1/f$  power spectrum will result in a Gaussian decay envelope [7, 9], flux-independent dephasing sources such as cavity-photon shot-noise [31–33] result in an exponential decay envelope. Ramsey decays for fixed-frequency qubits are therefore well fit with an exponential decay envelope. For all of our asymmetric transmons, as well as a large portion of the dephasing data for the  $\alpha = 1$  symmetric device, we find that an exponential decay envelope is also a good fit. In all of our data, we find that differences between values of  $T_2^*$  obtained using an exponential or Gaussian fit are systematic but slight. Furthermore, assuming a purely exponential decay simply puts an upper bound on the extracted flux noise level. A more complete discussion of the nature of our Ramsey decay envelopes and alternative fitting approaches appears in the Supplement.

Relaxation times  $T_1$  ranged from  $\sim 20 - 50 \mu\text{s}$  over the six qubits reported here. In general  $T_1$  increased with decreasing qubit frequency (Supplement, Fig. 2), consistent with dielectric loss and a frequency-independent loss tangent, as observed in other tunable superconducting qubits [34]. For the  $\alpha = 15$  qubit on sample B, a reduction in  $T_1$  with increasing frequency is also consistent with Purcell losses to the readout resonators. Qubits on sample A remained sufficiently detuned below the readout resonators that Purcell loss was not a significant loss channel.  $T_1$  relaxation due to coupling to a flux-bias line, as first discussed in [26] for a near symmetrical qubit, was considered for the higher asymmetry qubits studied here. We show in the Supplement that the upper bound on  $T_1$  due to the flux-line coupling for higher asymmetry qubits is not significantly lower than that reported in [26].

To compare dephasing rates among the qubits, we use the relation  $\Gamma_\phi = 1/T_2^* - 1/2T_1$  [35] to remove the contribution from the relaxation time. These values are plotted against flux in Fig. 3. As the curves in Fig. 2 illustrate, the integer and half-integer  $\Phi/\Phi_0$  points are ‘sweet spots’ where  $D_\Phi = 0$  and thus the qubit is first-order insensitive to flux noise. All the transmons on sample A clearly exhibit a dephasing rate that increases with  $D_\Phi$  and is a minimum at the sweet spots. Second-order sensitivity to flux noise [9, 36] should be negligible in our samples because of the small energy-band curvature. However, the level of  $\Gamma_\phi$  for the non-tunable qubit on each sample and the tunable qubits at their sweet spots indicates the presence of non-flux dependent sources of dephasing. Such background dephasing may arise from other mechanisms, including cavity-photon shot noise [31] or critical current noise [37]. This background dephasing may be expected to vary from qubit to qubit due to differences in qubit-cavity coupling or cavity thermalization, among other effects. Such variations are commonly observed in multi-qubit devices [3, 22, 28]. The Supplement contains dephasing data for additional devices similar to those discussed here, illustrating further variations in background dephasing.

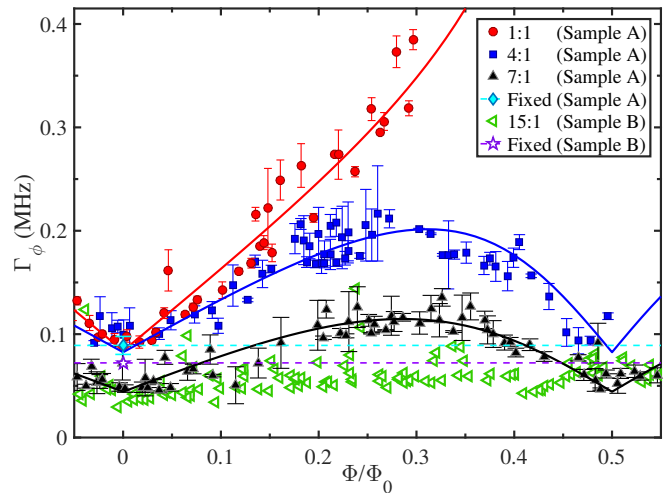


FIG. 3. (color online)  $\Gamma_\phi$  vs. flux measured for qubits from samples A and B. Solid lines show a simultaneous fit of the form  $mD_\Phi + b$  to the tunable qubits on sample A. Factor  $m$  is common to all three datasets while  $b$  is allowed to vary for each.  $\Gamma_\phi$  measured for fixed frequency qubits on both samples included with dashed lines to help guide the eye.

For sample A, if we consider only flux-dependent dephasing, it is evident that  $\Gamma_\phi \propto D_\Phi$ . Furthermore, qubits of the same geometry on the same chip should experience similar flux noise [14]. The analysis outlined in [7, 9] may then be used to extract a flux noise level from the relationship between  $\Gamma_\phi$  and  $D_\Phi$ . We apply a simultaneous fit of the form  $mD_\Phi + b$  to the  $\alpha = 1, 4$ , and  $7$  qubits, allowing background dephasing  $b$  to vary for each qubit, while a single  $m$  is common to all. The fit appears as solid lines in Fig. 3. We derive  $\Gamma_\phi = 2\pi\sqrt{A_\Phi|\ln(2\pi f_{IR}t)|}D_\Phi$  following the approach in Ref. [9], where the flux noise power spectrum is  $S_\Phi(f) = A_\Phi/|f|$ ,  $f_{IR}$  is the infrared cutoff frequency, which we take to be 1 Hz and  $t$  is on the order of  $1/\Gamma_\phi$ , which we take to be  $10 \mu\text{s}$  in our calculations. Using this equation, we can calculate the flux noise level impacting the qubits on sample A from the simultaneous fit parameter  $m$ . To determine the uncertainty in the measured flux noise level, we must not only account for the error in fitting  $m$  but also how variations in dephasing time impact the calculation of  $A_\Phi$  values from  $\Gamma_\phi$  and  $D_\Phi$  data. To account for the latter, we determine the impact on  $A_\Phi^{1/2}$  as  $t$  is varied. Adjusting  $t$  over a range similar to what we observe experimentally leads to a roughly 10% change  $A_\Phi^{1/2}$ . The errors we report for all calculated  $A_\Phi^{1/2}$  reflect this added uncertainty. We find that  $A_\Phi^{1/2} = 1.4 \pm 0.2 \mu\Phi_0$  on sample A. This level is compatible with previous experimental studies of flux noise in superconducting flux [6–8, 38, 39] and phase qubits [40].

To achieve an even clearer picture of the influence of flux noise on these qubits, we re-plot  $\Gamma_\phi$  vs.  $D_\Phi$  directly for each qubit in Fig. 4a. Here,  $D_\Phi$  is computed from the

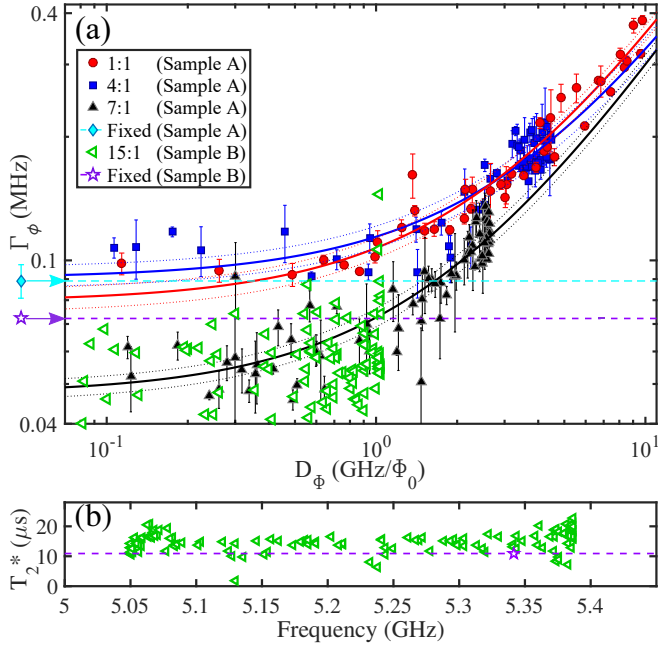


FIG. 4. (color online) (a)  $\Gamma_\phi$  vs.  $D_\phi$  measured for qubits from samples A and B. Solid lines show individual linear fits to the tunable qubits on sample A, as described in text. Note the scale is log-log.  $\Gamma_\phi$  measured for fixed-frequency qubits on both samples, included with dashed lines to help guide the eye. (b)  $T_2^*$  vs. frequency measured for the  $\alpha = 15$  and fixed-frequency qubits on sample B.

fits to the energy bands of each qubit shown in Fig. 2. This yields a linear dependence where the slope can be related to the amplitude of the flux noise and the offset corresponds to the background dephasing level. In this case, instead of a simultaneous fit we apply a separate fit of  $\Gamma_\phi = mD_\phi + b$  to each qubit, and we find  $A_\Phi^{1/2}$  values of  $1.3 \pm 0.2$ ,  $1.2 \pm 0.2$  and  $1.4 \pm 0.2$   $\mu\Phi_0$  for the  $\alpha = 7$ , 4 and 1 qubits, respectively. These flux noise levels are all consistent with past studies of low-frequency flux noise in superconducting devices [6–8, 38–40].

In Fig. 4a it can be seen that, for the tunable qubits on sample A, within the range  $D_\phi \lesssim 1$  GHz/ $\Phi_0$ , the measured dephasing rate is largely flux-independent within the experimental spread. To exploit this insensitivity, we designed the tunable transmon on sample B to have  $D_\phi$  no greater than  $\sim 1$  GHz/ $\Phi_0$  at any point within its tuning range, a condition satisfied by having  $\alpha = 15$ . As a result, its sensitivity to  $1/f$  flux noise appears to be suppressed below the level where background dephasing dominates.  $\Gamma_\phi$  is essentially flat across the entire tuning range, as shown in Fig. 3, with a mean of 58 kHz and experimental scatter of  $\sigma = 17$  kHz. In comparison, this sample’s fixed-frequency qubit exhibits  $\Gamma_\phi = 72$  kHz. Figure 4b shows clearly that  $T_2^*$  for the  $\alpha = 15$  qubit on sample B is independent of frequency over the whole tuning range.

Although no significant flux dependence of the dephasing is detectable for sample B, we estimate from our earlier expression for  $\Gamma_\phi$  that the observed scatter is consistent with  $A_\Phi^{1/2}$  of  $0.9$   $\mu\Phi_0$ . Recent progress in understanding the origins of  $1/f$  flux noise in SQUIDs [41] has facilitated up to a  $5\times$  reduction in  $A_\Phi$  [42]. Such reductions applied to the sample B qubit would reduce its maximum flux-noise-driven dephasing below 8 kHz. In a  $\alpha = 7$  qubit tunable over more than 700 MHz, flux noise of such a level would cause dephasing no greater than 17 kHz. Alternatively, in a qubit of 150 MHz tunability, the flux noise seen in sample B would cause dephasing not exceeding 8 kHz, or only 4 kHz if the flux noise were reduced as in Ref. [42]. We may contrast these values with the non-flux-noise-driven dephasing seen in state-of-the-art single-junction transmons used for multi-qubit gate operations:  $\Gamma_\phi = 4$  to 8 kHz on 2-qubit samples [23, 43], 10 kHz on 5-qubit samples [29] and 10 to 21 kHz on 7-qubit samples [28].

In conclusion, we have shown that by reducing the flux-tunability of a transmon qubit, we can dramatically lower its sensitivity to  $1/f$  flux noise. Using this understanding, we have fabricated a qubit in which the dephasing rate due to flux noise is suppressed below the level set by non-flux dependent sources. This device exhibits a flux-independent dephasing rate  $\Gamma_\phi \sim 60$  kHz over a tunable range in excess of 300 MHz. This qubit design should be readily adaptable to existing architectures aimed at the realization of a logically-encoded qubit, in both frequency-tuned gates and all-microwave gates. As qubit architectures progress to more complex geometries, this work will enable the implementation of multi-qubit gates without frequency collisions impacting gate performance. This is a promising route to the creation of high-fidelity two-qubit gates for reaching fault tolerance, thus fundamentally improving the scalability of such systems for the creation of a universal quantum computer.

This research was funded by the Office of the Director of National Intelligence (ODNI), Intelligence Advanced Research Projects Activity (IARPA), through the Army Research Office under Grant No. W911NF-16-0114. The device fabrication was performed in part at the Cornell NanoScale Facility, a member of the National Nanotechnology Coordinated Infrastructure (NNIC) which is supported by the National Science Foundation under Grant ECCS-1542081. We thank Y.-K.-K. Fung, J. Rohrs and J. R. Rozen for experimental contributions, and thank M. Brink, J.M. Gambetta, E. Magesan, R. McDermott, D.C. McKay and S. Rosenblatt for helpful discussions.

- 
- [1] R. Barends, J. Kelly, A. Megrant, A. Veitia, D. Sank, E. Jeffrey, T. C. White, J. Mutus, A. G. Fowler, B. Campbell, Y. Chen, B. Chiaro, A. Dunsworth,

- C. Neill, P. O'Malley, P. Roushan, A. Vainsencher, J. Wenner, A. N. Korotkov, A. N. Cleland, and M. J. Martinis, *Nature (London)* **508**, 500 (2014).
- [2] J. Kelly, R. Barends, A. G. Fowler, A. Megrant, E. Jeffrey, T. C. White, D. Sank, J. Y. Mutus, B. Campbell, Y. Chen, Z. Chen, B. Chiaro, A. Dunsworth, I. C. Hoi, C. Neill, P. O'Malley, C. Quintana, P. Roushan, A. Vainsencher, J. Wenner, A. N. Cleland, and J. M. Martinis, *Nature (London)* **519**, 66 (2015).
- [3] A. D. Córcoles, E. Magesan, S. J. Srinivasan, A. W. Cross, M. Steffen, J. M. Gambetta, and J. M. Chow, *Nat. Commun.* **6** (2015).
- [4] J. M. Gambetta, J. M. Chow, and M. Steffen, *npj Quant. Inf.* **3**, 2 (2017).
- [5] A. G. Fowler, M. Mariantoni, J. M. Martinis, and A. N. Cleland, *Phys. Rev. A* **86**, 032324 (2012).
- [6] S. M. Anton, C. Müller, J. S. Birenbaum, S. R. O'Kelley, A. D. Fefferman, D. S. Golubev, G. C. Hilton, H. M. Cho, K. D. Irwin, F. C. Wellstood, G. Schön, A. Shnirman, and J. Clarke, *Phys. Rev. B* **85**, 224505 (2012).
- [7] F. Yoshihara, K. Harrabi, A. O. Niskanen, Y. Nakamura, and J. S. Tsai, *Phys. Rev. Lett.* **97**, 167001 (2006).
- [8] J. Bylander, S. Gustavsson, F. Yan, F. Yoshihara, K. Harrabi, G. Fitch, D. G. Cory, Y. Nakamura, J. S. Tsai, and W. D. Oliver, *Nat. Phys.* **7**, 565 (2011).
- [9] G. Ithier, E. Collin, P. Joyez, P. J. Meeson, D. Vion, D. Esteve, F. Chiarello, A. Shnirman, Y. Makhlin, J. Schrieffer, and G. Schon, *Phys. Rev. B* **72**, 134519 (2005).
- [10] E. Paladino, Y. M. Galperin, G. Falci, and B. L. Altshuler, *Rev. Mod. Phys.* **86**, 361 (2014).
- [11] J. M. Martinis, S. Nam, J. Aumentado, K. M. Lang, and C. Urbina, *Phys. Rev. B* **67**, 094510 (2003).
- [12] F. C. Wellstood, C. Urbina, and J. Clarke, *Appl. Phys. Lett.* **50**, 772 (1987).
- [13] C. M. Quintana, Y. Chen, D. Sank, A. G. Petukhov, T. C. White, D. Kafri, B. Chiaro, A. Megrant, R. Barends, B. Campbell, Z. Chen, A. Dunsworth, A. G. Fowler, R. Graff, E. Jeffrey, J. Kelly, E. Lucero, J. Y. Mutus, M. Neeley, C. Neill, P. J. J. O'Malley, P. Roushan, A. Shabani, V. N. Smelyanskiy, A. Vainsencher, J. Wenner, H. Neven, and J. M. Martinis, *Phys. Rev. Lett.* **118**, 057702 (2017).
- [14] S. Sendelbach, D. Hover, A. Kittel, M. Mück, J. M. Martinis, and R. McDermott, *Phys. Rev. Lett.* **100**, 227006 (2008).
- [15] L. Faoro and L. B. Ioffe, *Phys. Rev. Lett.* **100**, 227005 (2008).
- [16] H. Wang, C. Shi, J. Hu, S. Han, C. Y. Clare, and R. Q. Wu, *Phys. Rev. Lett.* **115**, 077002 (2015).
- [17] S. LaForest and R. de Sousa, *Phys. Rev. B* **92**, 054502 (2015).
- [18] L. DiCarlo, J. M. Chow, J. M. Gambetta, L. S. Bishop, B. R. Johnson, D. I. Schuster, J. Majer, A. Blais, L. Frunzio, S. M. Girvin, and S. R. J, *Nature (London)* **460**, 240 (2009).
- [19] J. M. Martinis and M. R. Geller, *Phys. Rev. A* **90**, 022307 (2014).
- [20] C. Rigetti and M. Devoret, *Phys. Rev. B* **81**, 134507 (2010).
- [21] J. M. Chow, A. D. Córcoles, J. M. Gambetta, C. Rigetti, B. R. Johnson, J. A. Smolin, J. R. Rozen, G. A. Keefe, M. B. Rothwell, M. B. Ketchen, *et al.*, *Phys. Rev. Lett.* **107**, 080502 (2011).
- [22] J. M. Chow, J. M. Gambetta, E. Magesan, D. W. Abraham, A. W. Cross, B. R. Johnson, N. A. Masluk, C. A. Ryan, J. A. Smolin, S. J. Srinivasan, *et al.*, *Nat. Commun.* **5** (2014).
- [23] S. Sheldon, E. Magesan, J. M. Chow, and J. M. Gambetta, *Phys. Rev. A* **93**, 060302 (2016).
- [24] J. M. Gambetta, "Control of Superconducting Qubits." in *Quantum Information Processing*, Lecture Notes of the 44th IFF Spring School 2013, edited by D. DiVincenzo (2013) Chap. B4.
- [25] Private communication with S. Rosenblatt.
- [26] J. Koch, M. Y. Terri, J. Gambetta, A. A. Houck, D. I. Schuster, J. Majer, A. Blais, M. H. Devoret, S. M. Girvin, and R. J. Schoelkopf, *Phys. Rev. A* **76**, 042319 (2007).
- [27] J. D. Strand, M. Ware, F. Beaudoin, T. A. Ohki, B. R. Johnson, A. Blais, and B. L. T. Plourde, *Phys. Rev. B* **87**, 220505 (2013).
- [28] M. Takita, A. D. Córcoles, E. Magesan, B. Abdo, M. Brink, A. Cross, J. M. Chow, and J. M. Gambetta, *Phys. Rev. Lett.* **117**, 210505 (2016).
- [29] IBM Quantum Experience, <http://www.research.ibm.com/quantum/> (2017).
- [30] M. D. Reed, L. DiCarlo, B. R. Johnson, L. Sun, D. I. Schuster, L. Frunzio, and R. J. Schoelkopf, *Phys. Rev. Lett.* **105**, 173601 (2010).
- [31] A. P. Sears, A. Petrenko, G. Catelani, L. Sun, H. Paik, G. Kirchmair, L. Frunzio, L. Glazman, S. M. Girvin, and R. J. Schoelkopf, *Phys. Rev. B* **86**, 180504 (2012).
- [32] D. I. Schuster, A. Wallraff, A. Blais, L. Frunzio, R. S. Huang, J. Majer, S. M. Girvin, and R. J. Schoelkopf, *Phys. Rev. Lett.* **94**, 123602 (2005).
- [33] J. Gambetta, A. Blais, D. I. Schuster, A. Wallraff, L. Frunzio, J. Majer, M. H. Devoret, S. M. Girvin, and R. J. Schoelkopf, *Phys. Rev. A* **74**, 042318 (2006).
- [34] R. Barends, J. Kelly, A. Megrant, D. Sank, E. Jeffrey, Y. Chen, Y. Yin, B. Chiaro, J. Mutus, C. Neill, P. O'Malley, P. Roushan, J. Wenner, T. C. White, A. N. Cleland, and J. M. Martinis, *Phys. Rev. Lett.* **111**, 080502 (2013).
- [35] Y. Makhlin, G. Schön, and A. Shnirman, *Rev. Mod. Phys.* **73**, 357 (2001).
- [36] Y. Makhlin and A. Shnirman, *Phys. Rev. Lett.* **92**, 178301 (2004).
- [37] D. J. Van Harlingen, T. L. Robertson, B. L. T. Plourde, P. A. Reichardt, T. A. Crane, and J. Clarke, *Phys. Rev. B* **70**, 064517 (2004).
- [38] J.-L. Orgiazzi, C. Deng, D. Layden, R. Marchildon, F. Kitapli, F. Shen, M. Bal, F. R. Ong, and A. Lupascu, *Phys. Rev. B* **93**, 104518 (2016).
- [39] M. Stern, G. Catelani, Y. Kubo, C. Grezes, A. Bienfait, D. Vion, D. Esteve, and P. Bertet, *Phys. Rev. Lett.* **113**, 123601 (2014).
- [40] R. C. Bialczak, R. McDermott, M. Ansmann, M. Hofheinz, N. Katz, E. Lucero, M. Neeley, A. D. O'Connell, H. Wang, A. N. Cleland, *et al.*, *Phys. Rev. Lett.* **99**, 187006 (2007).
- [41] S. Sendelbach, D. Hover, M. Mück, and R. McDermott, *Phys. Rev. Lett.* **103**, 117001 (2009).
- [42] P. Kumar, S. Sendelbach, M. A. Beck, J. Freeland, Z. Wang, H. Wang, C. C. Yu, R. Q. Wu, D. P. Pappas, and R. McDermott, *Phys. Rev. Appl.* **6**, 041001 (2016).
- [43] S. Sheldon, L. S. Bishop, E. Magesan, S. Filipp, J. M. Chow, and J. M. Gambetta, *Phys. Rev. A* **93**, 012301 (2016).